JOURNAL OF COMPUTATIONAL PHYSICS 121, 314–323 (1995)

Study of Electron–Molecule Collision via Finite-Element Method and R-Matrix Propagation Technique: Exact Exchange

FARZAN ABDOLSALAMI

Department of Engineering Science, Trinity University, San Antonio, Texas 78212

MEHRAN ABDOLSALAMI, LENNARD PEREZ, AND PEDRO GOMEZ

Engineering Department, St. Mary's University, San Antonio, Texas 78228

AND

MARK SILVA

Department of Engineering Science, Trinity University, San Antonio, Texas 78212

Received December 2, 1994; revised March 21, 1995

We have applied the finite-element method to electron–molecule collision with the exchange effect implemented rigorously. All the calculations are done in the body-frame within the fixed-nuclei approximation, where the exact treatment of exchange as a nonlocal effect results in a set of coupled integro-differential equations. The method is applied to e-H_2 and e-N_2 scatterings and the cross sections obtained are in very good agreement with the corresponding results we have generated from the linear-algebraic approach. This confirms the significant difference observed between our results generated by linear-algebraic method and the previously published e-N_2 cross sections (M. A. Morrison and B. C. Saha, *Phys. Rev. A* **36**, 3682, 1987). Our studies show that the finite-element method is clearly superior to the linear-algebraic approach in both memory usage and CPU time especially for large systems such as e-N_2. The system coefficient matrix obtained from the finite-element method is often sparse and smaller in size by a factor of 12 to 16, compared to the linear-algebraic technique. Moreover, the CPU time required to obtain stable results with the finite-element method is significantly smaller than the linear-algebraic approach for one incident electron energy. The usage of computer resources in the finite-element method can even be reduced much further when (1) scattering calculations involving multiple electron energies are preformed in one computer run and (2) exchange, which is a short range effect, is approximated by a sparse matrix.

I. INTRODUCTION

The finite-element method (FEM) [1–3] is proven to be a very powerful technique to solve problems in all areas of engineering and physics. These problems, which are commonly described by differential, integral, integro-differential, or variational equations over a given domain, can be solved by the FEM even for the most complicated boundary conditions. This method divides the domain of interest into small subdomains called elements. Within each element, the solutions to the governing system equations are approximated by a linear combination of simple functions such as polynomials. The expansion coefficients within each element are then found such that a predefined residual error associated with this approximation is minimized while the global boundary conditions of the problem are satisfied.

In recent years, the FEM has been applied to scattering problems in atomic and molecular physics [4–6]. The major drawback of the FEM in these problems is the implementation of the K-matrix boundary conditions [7]. These boundary conditions extend the domain for the FEM analysis all the way into the asymptotic region, where the analytical form of the electronic wave function is known. In this case, the number of elements required for the study is large, resulting in a huge linear algebraic system equations that must be solved for the expansion coefficients in each element. The system equations obtained from the FEM are usually sparse and can be solved economically. However, for large molecules with multichannel scattering, the K-matrix boundary conditions still pose a severe demand on computer memory making FEM computationally prohibitive.

The FEM and R-matrix propagation technique have been combined recently to significantly reduce the memory demand in scattering studies [8]. In this approach, the R-matrix boundary conditions are imposed at the maximum radial distance occupied by most of the charge cloud of the molecule. This reduces the domain for FEM analysis by at least one order of magnitude compared to the K-matrix boundary conditions. Therefore, the number of elements used in implementing the R-matrix bound-

0021-9991/95 $12.00

ary conditions is small and the size of the linear-algebraic system equations obtained is manageable. This makes FEM very competitive with other numerical techniques available to study scattering problems.

In our previous work [8], the FEM and R-matrix propagation technique were applied to electron–molecule collision using model exchange. In the work presented here, we employ this approach to study exact exchange implementation in these collisions. In the body-frame within the fixed-nuclei approximation, this amounts to solving coupled integro-differential radial equations. We apply our method to e-H_2 and e-N_2 systems and compare our cross sections with those we have obtained from the linear-algebraic (LA) method. We also compare our e-N_2 cross sections with the previously published results [9]. This comparison shows significant differences in cross sections especially near the Π_g resonance energies. We discuss the memory and CPU time requirements of the two approaches and show that to obtain results which are in agreement to within 1%, the FEM is superior to the LA approach in using computer resources.

The material in this paper is arranged in the following order. In Section II, we discuss the scattering equations appropriate to electron–molecule systems with the exchange effect implemented rigorously. Section III covers the FEM implementation of the resulting BF-FN radial equation and its advantages over a few other techniques that implement exact exchange. We compare our FEM and LA results for the e-H_2 and e-N_2 systems in Section IV and discuss the differences between the new and previously published e-N_2 cross sections. Finally, Section V compares the use of computer resources for the two codes to obtain stable results.

II. SCATTERING THEORY

The body-frame fixed-nuclei (BF-FN) Schrodinger equation for electron–molecule collision has the form [7]

$$[\nabla^2 - 2V_{\text{int}}(\mathbf{r}, \mathbf{R}) + k_0^2]\mathbf{u}(\mathbf{r}, \mathbf{R}) = 0, \tag{1}$$

where k_0^2 and $\mathbf{u}(\mathbf{r}, \mathbf{R})$ are the energy and wave function of the scattering electron, respectively. In (1), $\mathbf{r}$ represents the position vector of the scattering electron with respect to the center of mass of the nuclei and $\mathbf{R}$ is the vector representing the internuclear separation of the target. The interaction potential between the scattering electron and the target molecule is represented by $V_{\text{int}}(\mathbf{r}, \mathbf{R})$. This potential can be written in terms of its static, polarization, and exchange components as

$$V_{\text{int}}(\mathbf{r}, \mathbf{R}) = V_{\text{st}}(\mathbf{r}, \mathbf{R}) + V_{\text{pol}}(\mathbf{r}, \mathbf{R}) + V_{\text{ex}}(\mathbf{r}, \mathbf{R}). \tag{2}$$

Static potential results from the coulomb interaction between the scattering electron and the constituent electrons and nuclei of the target molecule. This potential term is implemented here by averaging the coulomb potential energy over the $X^1\Sigma_g^+$ wave function [10].

For polarization, we use an *ab initio* potential developed by Gibson and Morrison [11]. This polarization potential, $V_{\text{pol}}(\mathbf{r}, \mathbf{R})$, is determined from self-consistant-field (SCF) calculations, where the induced polarization is determined as the difference between two energy-optimized functionals of an adiabatic electron–molecule Hamiltonian. With the scattering electron fixed in space, these two functionals correspond to polarized and unpolarized target wave functions, respectively. The nonadiabatic effects are then incorporated using a nonpenetrating approximation originally introduced by Temkin [12]. The polarization potential has the asymptotic form

$$V_{\text{pol}}(\mathbf{r}, \mathbf{R}) \sim -\frac{\alpha_0(\mathbf{R})}{2r^4} - \frac{\alpha_2(\mathbf{R})}{2r^4} P_2(\cos\theta), \tag{3}$$

where $\alpha_0(\mathbf{R})$ and $\alpha_2(\mathbf{R})$ are spherical and nonspherical polarizabilities, respectively.

The exchange effect is the result of explicitly imposing the antisymmetrization requirement of the Pauli principle on the system wave function. This potential term has the form [7]

$$V_{\text{ex}}(\mathbf{r}, \mathbf{R})\mathbf{u}(\mathbf{r}, \mathbf{R}) = \int K(\mathbf{r}, \mathbf{r}')\mathbf{u}(\mathbf{r}', \mathbf{R})\, d\mathbf{r}', \tag{4}$$

where

$$K(\mathbf{r}, \mathbf{r}') = -\sum_{i=1}^{N_{\text{occ}}} \Phi^i(\mathbf{r})|\mathbf{r} - \mathbf{r}'|^{-1}\Phi^{i*}(\mathbf{r}'). \tag{5}$$

In this equation, $\Phi^i(\mathbf{r})$ is the ith molecular orbital and N_{occ} is the number of occupied orbitals.

Expanding the scattering electron wave function, molecular orbitals, interaction potentials, and the $|\mathbf{r} - \mathbf{r}'|^{-1}$ term in these equations in terms of spherical harmonics and Legendre polynomials and integrating over the angular variables transform Eq. (1) to its desired coupled radial form [7, 9]

$$\left[\frac{d^2}{dr^2} - \frac{l(l+1)}{r^2} + k_0^2\right] u_{ll_0}^{\Lambda}(r) = 2\sum_{l'}^{l_{\max}} V_{ll'}^{\Lambda}(r) u_{l'l}^{\Lambda}(r) - 2\sum_{l''}^{l_{\max}^{\text{ex}}} \int K_{ll''}^{\Lambda}(r, r') u_{l''l_0}^{\Lambda}(r')\, dr', \tag{6}$$

where Λ is the projection of the angular momentum along the internuclear axis ($\hat{z}$ axis), l is the orbital angular momentum of the scattering electron, and l_0 designates a particular linearly independent solution. In this equation, $V_{ll'}^{\Lambda}(r)$ is the coupling matrix element associated with the static and polarization potentials. This term can be expressed in terms of the Clebsh–Gordan coefficients [13] and the expansion coefficients of these two potentials in terms of Legendre polynomials, $v_\lambda(r)$, as [9]

$$V^{\Lambda}_{ll'}(r) = \left(\frac{2l'+1}{2l+1}\right)^{1/2} \sum_{\lambda=0}^{\lambda_{\max}} v_\lambda(r) C(l'\lambda l; \Lambda 0) C(l'\lambda l; 00), \quad (7)$$

with λ denoting the order of a particular Legendre polynomials. The exchange kernel $K^{\Lambda}_{ll'}(r, r')$ is given by [7]

$$K^{\Lambda}_{ll'}(r, r') = \sum_{i=1}^{N_{\text{occ}}} \sum_{\lambda=0}^{\lambda_{\max}} \sum_{l''l'''}^{l^{\text{ex}}_{\max}} g_\lambda(ll'l''l'''|mm_i)\phi^i_{l''m_i}(r)\phi^{i*}_{l'''m_i}(r')\frac{r^\lambda_<}{r^{\lambda+1}_>}, \quad (8)$$

where

$$g_\lambda(ll'l''l'''|mm_i) = \left(\frac{(2l+1)(2l'+1)}{(2l''+1)(2l'''+1)}\right)^{1/2} C(0\lambda l''; -m, m-m_i) \times C(l\lambda l''; 00) C(l'\lambda l''; m, m_{i-m}) C(l'\lambda l'''; 00), \quad (9)$$

and $r_<$ ($r_>$) is the minimum (maximum) of r and r'. The maximum order of partial waves included in the scattering equation and its exchange term are $l_{\max}$ and $l^{\text{ex}}_{\max}$, respectively. These two terms may not have the same values because convergence can be achieved with a smaller number of partial waves included for the exchange interaction. Note that the **R** coordinate is suppressed in Eq. (6) since the rigid-rotor approximation is used which treats **R** as a parameter fixed at its equilibrium value. Equation (6) represents the standard BF-FN radial equations with the exchange effect implemented rigorously. These coupled integro-differential equations relate superposition of the wave function with weights $K^{\Lambda}_{ll'}(r, r')$ over the entire domain of interest to its value at a given point. The objective of this work is to solve these equations via the finite-element method to obtain the R-matrix which can then be propagated into the asymptotic region to find the K-matrix and scattering cross sections [14].

III. FINITE-ELEMENT ANALYSIS OF THE BF-FN RADIAL EQUATIONS

The BF-FN radial equations expressed in Eq. (6), which treat exchange as a nonlocal effect, involve the integral of the wave function over the domain of interest. In case of the R-matrix boundary conditions [7], this domain extends up to $r = a$ which defines the maximum radial distance occupied by most of the charge cloud of the molecule where the interaction potential is strong. The R-matrix boundary conditions for this problem are as follows [8]: at $r = 0$, $u^{\Lambda}_{ll_0}(r)$ is the zero matrix; at $r = a$, $\partial u^{\Lambda}_{ll_0}(r)/\partial r$ is the identity matrix. Since $u^{\Lambda}_{ll_0}(r = a)$ is the R-matrix, it can then be propagated into the asymptotic region to obtain the K-matrix and scattering cross sections.

The finite element model applied to this problem is based on the Galerkin method [1]. The wave function $u^{\Lambda}_{ll_0}(r)$ in any element is approximated by

$$u^{\Lambda}_{ll_0}(r) = \sum_{\alpha=1}^{2} (\phi_\alpha(x) u^{\Lambda}_\alpha + \bar{\phi}_\alpha(x) \bar{u}^{\Lambda}_\alpha), \quad 0 \le x \le 1, \quad (10)$$

where

$$\phi_\alpha(x) = \begin{cases} 2x^3 - 3x^2 + 1, & \alpha = 1, \\ 3x^2 - 2x^3, & \alpha = 2, \end{cases} \quad (11)$$

and

$$\bar{\phi}_\alpha(x) = \begin{cases} x^3 - 2x^2 + x, & \alpha = 1, \\ x^3 - x^2, & \alpha = 2, \end{cases} \quad (12)$$

define the basis for the expansion of the wave function in every element. In Eq. (10), $x = 0, 1$ represent the end points of any element with the actual radial distance r within an element given by $r = (n-1)h + hx$, where n is the element index and h is the mesh size. These definitions force u^{Λ}_α and $\bar{u}^{\Lambda}_\alpha$ to be the values of the wave function and its derivative at the end points of an element ($x = 0, 1$).

To implement FEM using R-matrix boundary conditions, we multiply Eq. (6) by each of the basis functions ϕ_α and $\bar{\phi}_\alpha$ and integrate in the range $r = 0$ to a. We now have

$$\int_{r=0}^{a} \left\{ \left[\frac{d^2}{dr^2} - \frac{l(l+1)}{r^2} + k_0^2 \right] u^{\Lambda}_{ll_0}(r) - 2 \sum_{l'}^{l_{\max}} V_{ll'}(r) u^{\Lambda}_{l'l}(r) \right\} \phi^i(x)\, dr + 2 \int_{r=0}^{a} \left[\int_{r'=0}^{a} \sum_{l''}^{l^{\text{ex}}_{\max}} K_{ll''}(r, r') u^{\Lambda}_{l''l_0}(r')\, dr' \right] \phi^i(x)\, dr = 0, \quad (13)$$

where $\phi^i(x)$ ($i = 1, 4$) represents any of the basis functions ϕ_α and $\bar{\phi}_\alpha$.

The integrals in Eq. (13) are discretized into N small elements and within each element, $u^{\Lambda}_{ll_0}(r)$ is approximated by Eq. (10). Once each integral over an element is evaluated, the results can be added together to obtain the homogenous equations $\mathbf{AU} = 0$ which approximates Eq. (6). The first integral term in Eq. (13), which breaks down to single integrals over elements, transforms into a coefficient matrix of size $(2N + 2)m$, where N is the total number of elements in the finite-element analysis and m is the number of coupled equations. This matrix is sparse and can be divided into m^2 partitions of diagonal matrices with a bandwidth of three. Each partition would then represent the

contribution of one of the radial wave functions, $u^{\lambda}_{l l_0}(r)$, to the overall set of coupled differential equations. Discretizing the second integral term in Eq. (13) results in double integrals that extend over different elements n and np such that $r = (n - 1)h + hx$ and $r' = (np - 1)h + hy$. In other words, the nonlocal exchange effect causes different elements to be coupled to each other. Substituting Eq. (10) into these double integrals and adding the results transform the second term in Eq. (13) into a full matrix of size $(2N + 2)p$, where p is the number of exchange channels. This implies that the matrix representation of exact exchange effect in FEM consists of p^2 partitions and is not sparse. The system coefficient matrix **A** is now obtained by adding the matrix representations of the two integral terms in Eq. (13). This system matrix has p^2 full partitions and $m^2 - p^2$ diagonal partitions with a bandwidth of three. If the number of exchange channels become equal to the number of channels in the scattering problem, the sparsity of **A** is completely lost. Implementation of the boundary conditions described before in the system equations $\mathbf{AU} = 0$ results in a set of nonhomogenous equations from which the R-matrix can be computed.

The finite-element method has two advantages over the very few other techniques that can solve the exact exchange BF-FN radial equations. These advantages are the CPU time and computer memory usage. The square coefficient matrix **A** can be written as

$$\mathbf{A} = \mathbf{A}_1 + k_0^2 \mathbf{A}_2, \tag{14}$$

where $\mathbf{A}_1$ is the matrix obtained from applying the finite-element method to all the terms in Eq. (13), except the electron energy term which is represented by $k_0^2\mathbf{A}_2$. From Eqs. (13) and (14), it is clear that since $\mathbf{A}_1$ and $\mathbf{A}_2$ are independent of the energy of the incident electron, they only need to be computed once for a given symmetry. Obtaining the coefficient matrix for multiple energies then amounts to the simple matrix operation defined in Eq. (14) which significantly reduces the CPU time. Moreover, exchange is a short-range effect which means that the exchange kernel $K^{\Lambda}_{ll'}(r, r')$ is significant only for a small r' domain about a given r value. In the finite-element code, we can ignore the double integrals obtained from discretizing the second integral term in Eq. (13) if the coupled elements n and np are different by more than a predefined threshold value. This has the effect of transforming the second integral term in this equation to a sparse matrix with p^2 partitions. These partitions are diagonal with a bandwidth that is dependent on the threshold value. The threshold value can then be systematically increased until the desired convergence in cross sections is achieved. This implies that in the FEM formulation exact exchange can be approximated by a sparse matrix. For molecules with a large number of channels, the memory and CPU time advantages of the finite-element method obtained from controlling the bandwidth of the exchange matrix is very significant.

IV. RESULTS

There are five parameters whose proper values are very critical in order to obtain stable cross sections. These parameters, three of which are the upper limits on various summations in the radial scattering Eqs. (6)–(8), are defined below:

1. $\lambda_{\max}$. The maximum order of the Legendre polynomials included in the expansion of the interaction potentials in Eqs. (7) and (8).
2. $l_{\max}$. The maximum order of the partial waves included in the BF-FN scattering equations.
3. $l^{\text{ex}}_{\max}$. The maximum order of the partial waves included in the exchange part of the BF-FN scattering equations.
4. $l^{\text{mo}}_{\max}$. The maximum order of the partial waves included in the expansion of the bound molecular orbitals in terms of spherical harmonics.
5. $r_{\max}$. The radial distance at which the K-matrix is extracted.

In what follows, we will present the cross sections obtained for electron-H_2 and electron-N_2 scatterings. The proper values of these parameters to assure the stability of the cross sections will also be discussed for these two systems.

A. e-H_2 *Systems*

We have applied the FEM and R-matrix propagation technique to electron-H_2 scattering. Table I shows the cross sections obtained using this method and the corresponding results from the LA approach for Σ and Π symmetries. In both calculations, we have used five channels ($m = p = 5$) with $r = a$ set to 10 bohr. These number of channels translate to $l_{\max} = l^{\text{ex}}_{\max} = 8 + l_{\min}$ with $l_{\min}$ determined by the symmetry. The K matrix is extracted at $r_{\max} = 130$ bohr with $l^{\text{mo}}_{\max} = 8$ and $\lambda_{\max} = 6$, 7, 8, and 7 for Σ_g, Σ_u, Π_g, and Π_u symmetries, respectively. The energy range used for comparison is 0.047 to 7.0 eV. From this table, it is clear that the results obtained from these two approaches are in agreement to within less than 1% for each energy and symmetry.

We have also taken advantage of the short range effect of exchange interaction to make its FEM matrix representation sparse. In our code, the p^2 partitions associated with this effect have been adjusted in bandwidth until the minimum required value to achieve stable results is obtained. Our investigation shows that exchange effect is significant (on an average sense) only if two coupled elements n and np differ by at most 3. With an average mesh size of 0.7 bohr for the e-H_2 system, this translates to an effective exchange interaction radii of about 2 bohr.

B. e-N_2 *Systems*

We have performed extensive convergence studies on e-N_2 cross sections for the four lowest BF-FN electron–molecule symmetries (Σ_g, Σ_u, Π_g, Π_u) at energies up to 1.0 Ry. We have

TABLE I

Calculated Values of the e-H_2 Cross Sections in Square Bohr from the Finite-Element and Linear-Algebraic Techniques

	Σ_g		Σ_u		Π_g		Π_u		Total	
E(eV)	LA	FEM	LA	FEM	LA	FEM	LA	FEM	LA	FEM
0.047	28.275	28.208	0.388	0.388	0.012	0.012	0.016	0.016	28.691	28.624
0.050	28.474	28.408	0.402	0.402	0.012	0.012	0.018	0.018	28.906	28.840
0.060	29.082	29.015	0.449	0.448	0.014	0.014	0.025	0.025	29.570	29.502
0.070	29.619	29.553	0.496	0.495	0.015	0.015	0.034	0.034	30.164	30.097
0.080	30.100	30.034	0.543	0.542	0.016	0.016	0.044	0.044	30.703	30.636
0.090	30.535	30.469	0.589	0.588	0.017	0.017	0.054	0.054	31.195	31.128
0.100	30.931	30.865	0.635	0.633	0.018	0.018	0.066	0.066	31.650	31.582
0.200	33.653	33.590	1.112	1.108	0.027	0.027	0.204	0.203	34.996	34.928
0.300	35.214	35.154	1.627	1.619	0.035	0.035	0.370	0.368	37.246	37.176
0.400	36.213	36.157	2.181	2.169	0.042	0.042	0.551	0.549	38.987	38.917
0.500	36.876	36.825	2.773	2.756	0.049	0.049	0.742	0.739	40.440	40.369
0.700	37.595	37.551	4.056	4.028	0.063	0.063	1.142	1.136	42.856	42.778
0.900	37.826	37.789	5.443	5.402	0.077	0.077	1.553	1.544	44.899	44.812
1.000	37.825	37.791	6.165	6.117	0.084	0.084	1.759	1.749	45.833	45.741
2.000	35.912	35.904	13.261	13.150	0.150	0.150	3.661	3.637	52.984	52.841
3.000	32.925	32.925	17.845	17.722	0.213	0.212	5.050	5.019	56.033	55.878
4.000	29.917	29.921	19.353	19.252	0.273	0.271	5.888	5.856	55.431	55.300
5.000	27.140	27.145	18.995	18.918	0.329	0.326	6.291	6.258	52.755	52.647
6.000	24.646	24.651	17.845	17.789	0.379	0.377	6.394	6.361	49.264	49.178
7.000	22.432	22.432	16.471	16.434	0.425	0.422	6.308	6.279	45.636	45.567

Note. All the results shown are based on five channels ($m = p = 5$) with $r = a$ set to 10 bohr. This table shows that for all symmetries, the results obtained from these two methods are in agreement to within less than 1%.

determined the minimum required values of the five parameters discussed earlier to obtain 1% accuracy in the cross sections *for each symmetry*. The proper values of l_{max}, l^{ex}_{max}, l^{mo}_{max}, and λ_{max} are given in Table II. To achieve the desired level of accuracy in the cross sections, r_{max} has to be set to 900 bohr [15].

Tables III and IV compare the cross sections we have calculated for the Σ_g, Σ_u, Π_g, and Π_u symmetries using FEM and LA approaches in the energy range 0.0007 to 1.0 Ry. In these tables, the FEM results are listed in two different columns. The column labeled FB refers to the case where the exchange part of Eq. (6) is represented by a matrix which has p^2 full partitions. The results obtained by enforcing sparsity into the exchange matrix are given in the column labeled PB (partial bandwidth).

TABLE II

The Convergence Parameters Used in the LA and FEM Calculations

Symmetry	l_{max}	l^{ex}_{max}	l^{mo}_{max}	λ_{max}
Σ_g	58	22	10	116
Σ_u	59	21	10	117
Π_g	32	20	10	62
Π_u	31	11	10	61

Note. These values are determined such that 1% accuracy in e-N_2 cross sections are obtained for each symmetry (Σ_g, Σ_u, Π_g, Π_u).

From these tables, it is clear that our results from FEM and LA approaches are in agreement to within less than 1% for each energy and symmetry. Our studies indicate that for the e-N_2 system, exchange is significant only if two coupled elements differ by at most 5. With an average mesh size of $\frac{1}{3}$, this translates to an effective exchange interaction radii of about 1.7 bohr.

In Figs. 1 through 5, we plot the Σ_g, Σ_u, Π_g, Π_u and total e-N_2 cross sections obtained from FEM. In these figures, we have also included the results published by Morrison and Saha [9]. It is evident from these graphs that there is a significant difference between the two results especially for Π_g symmetry near resonance. Note that for this symmetry the electron energy at which the maximum cross section is attained has shifted from 0.18 Ry in the previous calculations to 0.2 Ry in the FEM results. Since Π_g is the dominant symmetry in the energy range 0.15–0.23 Ry, this difference is also reflected in the total cross sections shown in Fig. 5. The discrepancy observed between the new and old e-N_2 cross sections is due to the difference in convergence parameters used in the scattering calculations [9, 16].

V. COMPARISON OF CPU TIME AND MEMORY USAGE

In this section, we compare FEM and LA techniques in terms of CPU time and memory usage required to obtain cross sections

TABLE III

Calculated Values of the e-N_2 Cross Sections (in Square Bohr) for Σ Symmetries Using Finite-Element Method with Full Bandwidth (FEM(FB)) and Partial Bandwidth (FEM(PB)) Implementations and the Linear-Algebraic (LA) Technique

	Σ_g			Σ_u		
E(Ry)	FEM(FB)	FEM(PB)	LA	FEM(FB)	FEM(PB)	LA
0.0007	5.435	5.389	5.420	0.191	0.191	0.191
0.0015	7.373	7.319	7.356	0.124	0.124	0.124
0.0029	9.844	9.783	9.825	0.070	0.070	0.070
0.0051	12.714	12.646	12.668	0.036	0.036	0.036
0.0100	17.151	17.074	17.102	0.014	0.014	0.014
0.0500	30.118	30.022	30.036	0.054	0.054	0.055
0.1000	33.460	33.361	33.395	0.491	0.489	0.491
0.1500	33.443	33.348	33.383	1.285	1.282	1.284
0.2000	32.285	32.197	32.236	2.237	2.233	2.228
0.2500	30.704	30.623	30.666	3.217	3.213	3.207
0.3500	27.271	27.208	27.253	5.024	5.019	5.011
0.5000	22.534	22.494	22.514	7.089	7.084	7.074
0.7500	16.562	16.546	16.563	8.994	8.934	8.982
1.0000	12.606	12.606	12.607	9.817	9.770	9.809

Note. All the results are converged to within 1% accuracy.

which are in agreement to within 1% for both e-H_2 and e-N_2 systems.

Computation of the system coefficient matrix as described in Eq. (14) can significantly reduce the CPU time in the FEM approach to obtain cross sections for more than one scattering electron energy. Once a new electron energy is introduced, the k_0^2 term in this equation is updated and the new R-matrix is found. The LA approach, on the other hand, is based on an integral form of the BF-FN radial equation obtained from the free-particle Green's function. The system coefficient matrix that results from this approach cannot be represented in a form similar to Eq. (14) with the energy term isolated. This implies that for different electron energies the entire system equations have to be recomputed resulting in a significantly higher CPU time compared to the FEM approach.

We can also take advantage of the short-range effect of

TABLE IV

Calculated Values of the e-N_2 Cross Sections (in Square Bohr) for Π Symmetries Using Finite-Element Method with Full Bandwidth (FEM(FB)) and Partial Bandwidth (FEM(PB)) Implementations and the Linear-Algebraic (LA) Technique

	Π_g			Π_u			Total		
E(Ry)	FEM(FB)	FEM(PB)	LA	FEM(FB)	FEM(PB)	LA	FEM(FB)	FEM(PB)	LA
0.0007	0.012	0.012	0.012	0.547	0.547	0.547	6.185	6.138	6.170
0.0015	0.009	0.009	0.009	0.722	0.722	0.722	8.228	8.174	8.211
0.0029	0.007	0.007	0.007	0.938	0.938	0.938	10.860	10.799	10.840
0.0051	0.007	0.007	0.007	1.170	1.171	1.171	13.926	13.859	13.881
0.0100	0.011	0.011	0.011	1.467	1.468	1.468	18.644	18.568	18.595
0.0500	0.235	0.235	0.236	1.164	1.168	1.167	31.572	31.479	31.493
0.1000	2.355	2.354	2.367	0.255	0.258	0.255	36.560	36.462	36.508
0.1500	34.276	34.240	34.402	0.039	0.039	0.039	69.043	68.909	69.108
0.2000	75.533	75.588	75.295	0.340	0.335	0.339	110.395	110.353	110.099
0.2500	21.999	22.007	21.829	0.931	0.924	0.931	56.851	56.767	56.633
0.3500	10.120	10.121	10.079	2.452	2.439	2.443	44.867	44.787	44.785
0.5000	7.343	7.343	7.332	4.715	4.698	4.703	41.682	41.619	41.623
0.7500	6.391	6.391	6.381	7.529	7.511	7.517	39.476	39.381	39.444
1.0000	6.057	6.057	6.048	9.293	9.277	9.283	37.774	37.710	37.747

Note. All the results are converged to within 1% accuracy. The total cross sections (summed over all symmetries) are also shown.

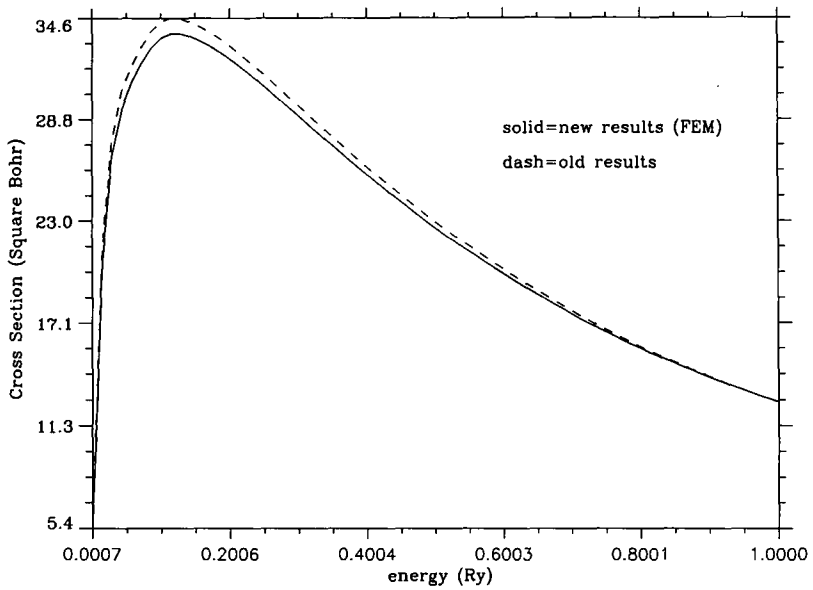

FIG. 1. Comparison of new (FEM—solid) and old (Morrison and Saha—dash) cross sections for the e-N_2 scattering in Σ_g symmetry.

exchange interaction to make its FEM matrix representation sparse and thereby to reduce the memory requirement. As mentioned before, the p^2 partitions within the coefficient matrix **A** which are related to exchange have adjustable bandwidths. These bandwidths can be set to the minimum required value such that the desired convergence in cross sections is achieved. This implies that within the FEM scheme we can approximate the full matrix representation of exact exchange with a sparse matrix without loss of accuracy. This approximation would significantly reduce the memory and CPU time requirement of the FEM method, especially for large systems such as e-N_2. In what follows, we discuss the CPU time and memory usage of FEM and LA approaches with and without the two advantages of FEM discussed above taken into account.

A. e-H_2 *Systems*

To obtain cross sections which are accurate to within 1%, the FEM and LA codes require full system coefficient matrices

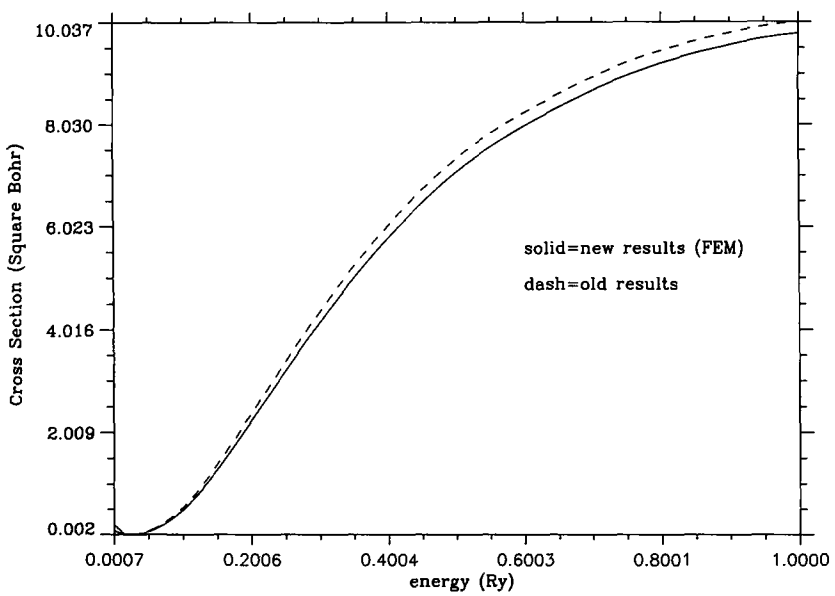

FIG. 2. Comparison of new (FEM—solid) and old (Morrison and Saha—dash) cross sections for the e-N_2 scattering in Σ_u symmetry.

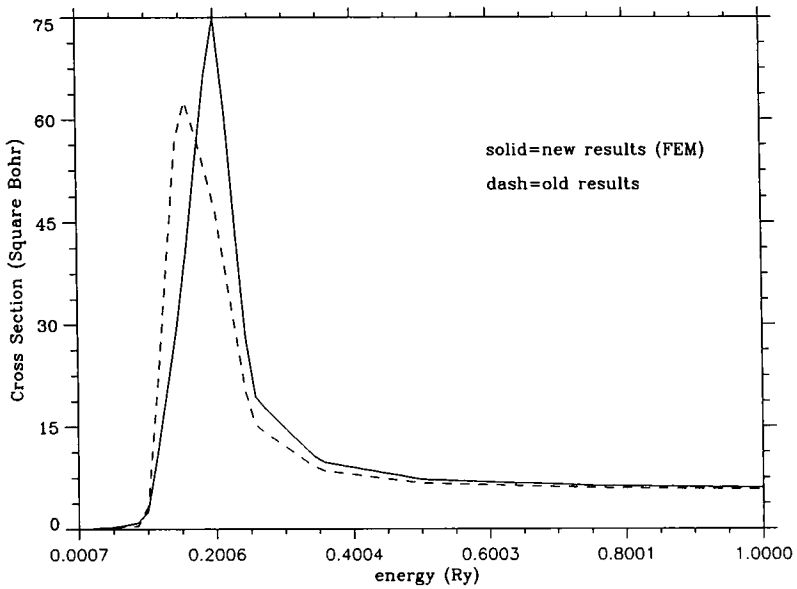

FIG. 3. Comparison of new (FEM—solid) and old (Morrison and Saha—dash) cross sections for the e-N_2 scattering in Π_g symmetry.

of sizes 150 and 275, respectively. On the average, the CPU time required for both codes to compute cross sections on a SPARC station 2 with 20 Mbytes of memory is less than 30 s for a given energy and symmetry. However, approximating exchange with a sparse matrix reduces the density of the FEM system matrix to 35%. Since nonzero elements are the only ones actually stored, this reduction in density translates to a reduction in the memory requirement. Moreover, FEM demands half the CPU time of the LA approach to compute cross sections for 20 energies and four symmetries in one computer run.

B. e-N_2 *Systems*

For a large system such as e-N_2, FEM is superior to the LA approach with or without the advantages of the FEM taken into account. Figure 6 compares the average CPU time requirements

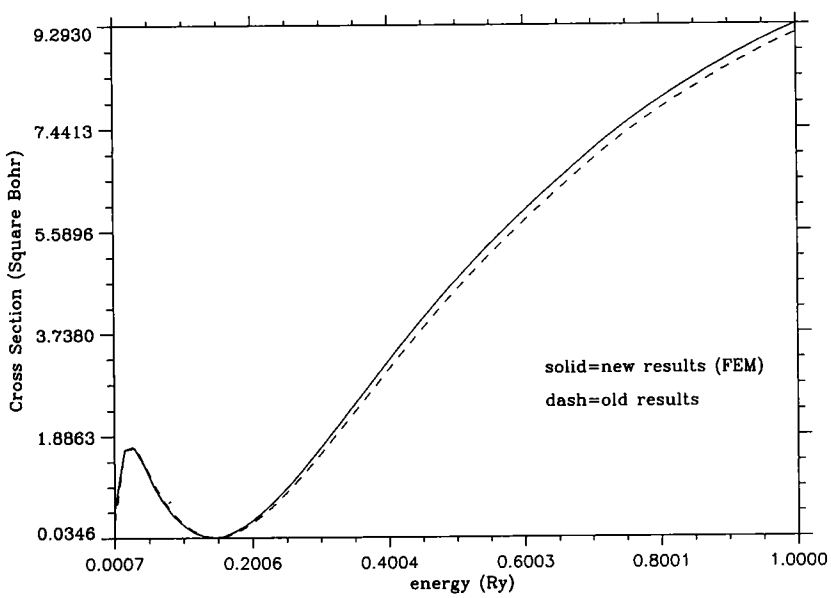

FIG. 4. Comparison of new (FEM—solid) and old (Morrison and Saha—dash) cross sections for the e-N_2 scattering in Π_u symmetry.

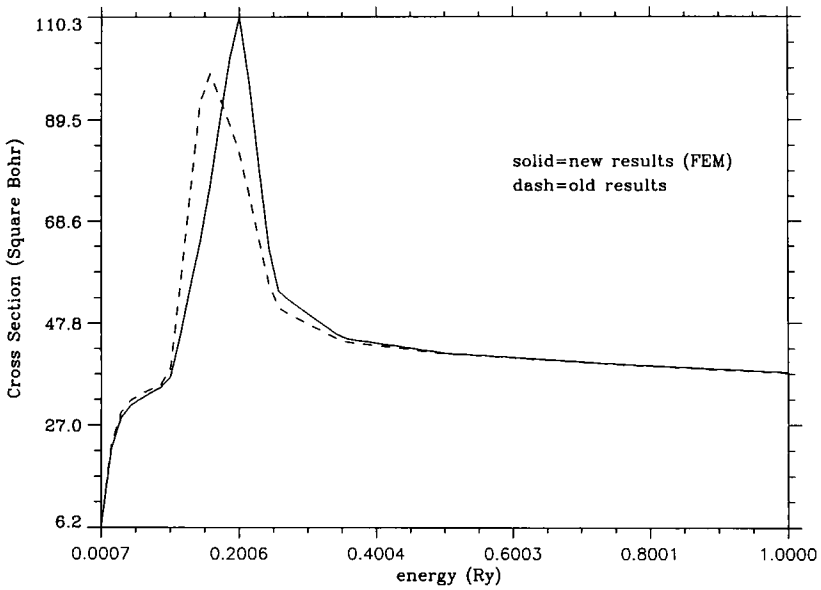

FIG. 5. Comparison of new (FEM—solid) and old (Morrison and Saha—dash) total cross sections for the e-N_2 system summed over the Σ and Π symmetries.

of the two codes to compute the cross section for one energy at one symmetry [17]. All the results shown in this figure pertain to a SPARC station 10 with four HyperSPARC processors and 160 Mbytes of memory. In Fig. 6, SE (single energy) refers to scattering calculations involving one electron energy at a time without taking advantage of Eq. (14). Scattering calculations involving multiple electron energies are denoted by ME (multiple energies). This figure shows that FEM is faster than LA approach by a factor of four even if scattering calculations involving a single electron energy and full matrix representation

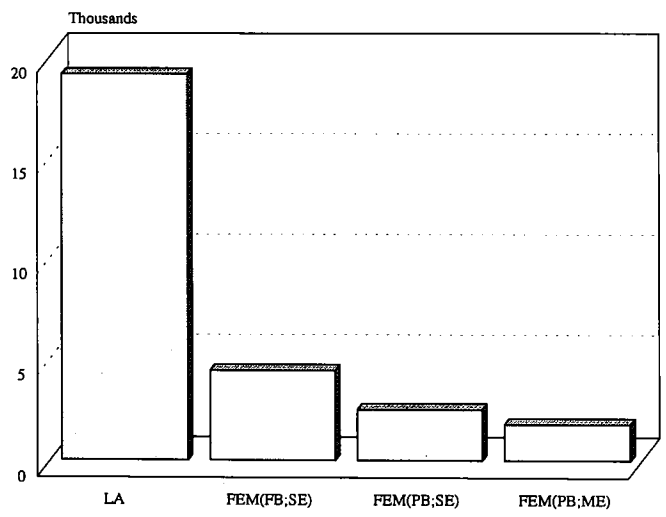

FIG. 6. The average CPU time requirement (in seconds) for the LA and FEM codes. The times are obtained by averaging the CPU times for Σ_g at 0.0007 Ry, Σ_g at 1.0 Ry, Π_g at 0.2 Ry, and Π_u at 1.0 Ry. All calculations are performed on a SPARCstation 10 with four HyperSPARC processors and 160 Mbytes of memory. The notations used in this figure are: LA = linear algebraic; FEM(FB;SE) = finite element with full bandwidth and single scattering electron energy; FEM(PB;SE) = finite element with partial bandwidth and single scattering electron energy; FEM(PB;ME) = finite element with partial bandwidth and multiple scattering electron energies.

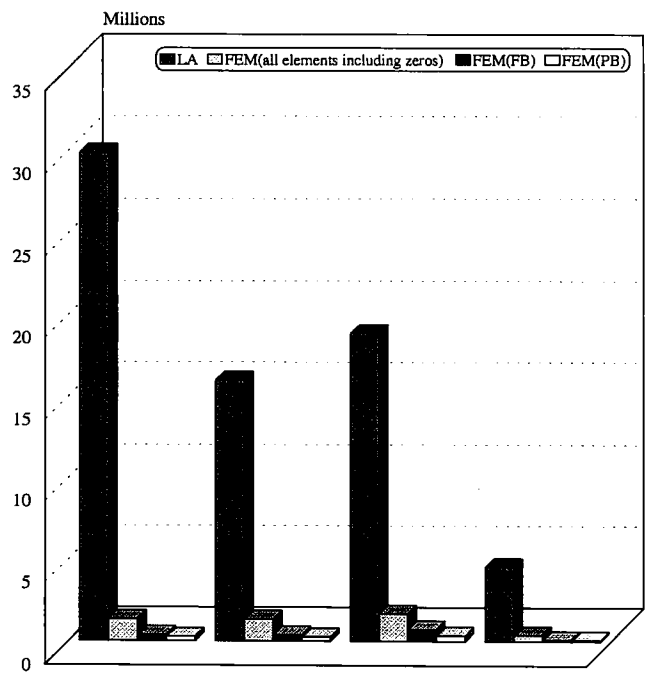

FIG. 7. Number of elements in the e-N_2 system matrix for FEM and LA methods as a function of energy and symmetry. In this figure, FEM(FB) and FEM(PB) refer to the full and partial bandwidth implementations of the finite element method.

TABLE V

The Size and Density of the e-N_2 System Matrix as a Function of Energy and Symmetry for the LA and FEM Codes

	LA		FEM(FB)		FEM(PB)	
Symmetry & energy	Size	Density	Size	Density	Size	Density
Σ_g@0.0007Ry	5460^2	100%	1140^2	27%	1140^2	19%
Σ_u@1.0000Ry	3990^2	100%	1140^2	27%	1140^2	19%
Π_g@0.2000Ry	4336^2	100%	1280^2	41%	1280^2	21%
Π_u@1.0000Ry	2128^2	100%	608^2	26%	608^2	20%

Note. Here, FB and PB represent the full and partial bandwidth implementations of the FEM method, respectively. The density gives the percentage of the nonzero elements in the system matrix that are actually stored.

of exchange are assumed. When the advantages of FEM are both taken into account, FEM is faster by a factor of 10, compared to the LA code.

Next, we compare the memory requirements of the two approaches to obtain stable results. Table V shows the size and density of the system matrix obtained for the e-N_2 system as a function of energy and symmetry. In this table, it is important to note that the density of the FEM system matrix is reduced when exchange is modeled by a sparse matrix. The number of nonzero elements in the system matrix which needs to be stored for each case is plotted in Fig. 7 for both FEM and LA methods. This figure shows that for large molecules such as N_2, the memory requirement of FEM is significantly less than the LA approach.

VI. CONCLUSION

We have applied the finite-element method and R-matrix propagation technique to study electron–molecule collision with exchange implemented rigorously. We find the cross sections for the e-H_2 and e-N_2 systems to be in agreement to within 1% with the results we have generated from the linear algebraic approach. The results we have obtained for e-N_2 cross sections are not in close agreement with those reported earlier by Morrison and Saha near Π_g resonance energies due to significant differences in values of the convergence parameters used in the two studies.

Our finite-element implementation of exact exchange points out two advantages of this method: (1) scattering calculations involving multiple electron energies can be carried out in one computer run to significantly reduce the CPU time and (2) exchange can be approximated by a sparse matrix which reduces the density of the FEM system matrix and thereby the memory requirement. We find that the CPU time and memory requirements of FEM are far less than the LA approach to obtain converged cross sections especially for e-N_2 system. As a result, we conclude that the combination of FEM and R-matrix propagation technique is a very efficient method in terms of computer resources to study electron–molecule scattering.

ACKNOWLEDGMENT

The authors thank Dr. Michael Morrison, Dr. J. Shertzer, Dr. Warren Buck, Dr. Brian Elza, Dr. Wayne Trail, and Dr. Bidhan Saha for their helpful discussions throughout this work. This work was supported by the National Science Foundation under Grant RII-9014116.

REFERENCES

1. J. E. Akin, *Finite Element Analysis for Undergraduates* (Academic Press, New York, 1986).
2. D. S. Burnett, *Finite Element Analysis* (Addison–Wesley, Menlo Park, CA, 1986).
3. H. Grandin Jr., *Fundamentals of the Finite Element Method* (Macmillan Co., New York, 1986).
4. L. R. Ram-Mohan, S. Saigal, D. Dossa, and J. Shertzer, *Comput. Phys.*, p. 50 (1990).
5. J. Botero and J. Shertzer, *Phys. Rev. A* **46,** R1155 (1992).
6. J. Shertzer and L. R. Ram-Mohan, *Phys. Rev. B* **41,** 9994 (1990).
7. L. A. Collins and B. I. Schneider, *Phys. Rev. A* **24,** 2387 (1981).
8. F. Abdolsalami, M. Abdolsalami, and P. Gomez, *Phys. Rev. A* **50,** 360 (1994).
9. M. A. Morrison and B. C. Saha, *Phys. Rev. A* **36,** 3682 (1987).
10. Y. Oksyuk and Z. E. T. Fiz, *Sov. Phys. JETP* **22,** 873 (1966).
11. T. L. Gibson and M. A. Morrison, *J. Phys. B* **15,** L221 (1982).
12. A. Temkin, *Phys. Rev.* **107,** 1004 (1957).
13. M. E. Rose, *Elementary Theory of Angular Momentum* (Wiley, New York, 1957).
14. J. C. Light and R. B. Walker, *J. Chem. Phys.* **65,** 4272 (1976).
15. To achieve 1% accuracy for the total cross sections (summed over Σ and Π symmetries), lower values of these convergence parameters are required. Moreover, r_{max} does not have to be nearly as high as 900 bohr for 1% accuracy at energies above threshold.
16. L. Perez and M. Abdolslami, in *Proceedings, Second National Conference on Diversity in the Scientific and Technological Workforce* (National Science Foundation, Washington, 1993).
17. To compute the average CPU time per energy and symmetry, we have used the CPU time for Σ_g at 0.0007 Ry, Σ_g at 1.0 Ry, Π_g at 0.2 Ry, and Π_u at 1.0 Ry. These particular energies and symmetries reflect the various CPU time and memory requirements we have incurred in our scattering calculations.